IJPAS | INTERNATIONAL JOURNAL PURE AND APPLIED SCIENCES
ISSN: 2149-0910
Vol. 10(2); 394-406 (2024)
DOI: 10.29132/ijpas.1501474

Research Article

BR 46 Adsorption Application: In Situ HF Production of $Ti_3C_2T_x$ via LiF/HCl Etching

Aytekin ÇELIK*, Umay HALISDEMIR, Yusuf KÖSE, Mustafa YEGIN

Received: 19.06.2024
Accepted: 22.12.2024

Fırat University, Faculty of Engineering, Department of Environmental Engineering, Elazig, Türkiye; aytekincelik@firat.edu.tr, umayhalisdemir@gmail.com, yusufkose99@hotmail.com, mustafa.yegin@outlook.com
* Corresponding author

Abstract: This study investigates the adsorption capabilities of $Ti_3C_2T_x$ MXene to remove Basic Red 46 (BR 46) dye from aqueous solutions. Azo dyes such as BR 46 are common pollutants from textile industries and pose significant ecological and health risks due to their toxicity and persistence. Current removal methods face efficiency issues affected by dye composition, pH, and other contaminants. Advanced oxidation processes (AOPs) and adsorption methods are promising but require optimization for practical application. MXenes, two-dimensional transition metal carbides/nitrides, offer high adsorption capacity and stability. In this study, the titanium aluminum carbide (Ti_3AlC_2) MAX phase was exfoliated using lithium fluoride (LiF)+hydrochloride acid (HCl) to synthesize $Ti_3C_2T_x$. Characterization techniques including Fourier transform infrared spectrometry (FTIR), X-ray diffraction (XRD), and scanning electron microscopy (SEM) were used to analyze the material. The study examined the effects of various reaction conditions such as pH, MXene dosage, and initial dye concentration on BR 46 adsorption. The results show that $Ti_3C_2T_x$ MXene is an effective adsorbent and provides a potential solution for removing toxic dyes from wastewater. This study contributes to developing efficient, cost-effective, and sustainable methods to reduce dye pollution in water resources.

Keywords: MXene; adsorption; azo dye; LiF/HCl

Araştırma makalesi

BR 46 Adsorpsiyon Uygulaması: LiF/HCl Aşındırma Yoluyla $Ti_3C_2T_x$'nin Yerinde HF Üretimi

Özet: Bu çalışma, $Ti_3C_2T_x$ MXene'in sulu çözeltilerden Basic Red 46 (BR 46) boyasını uzaklaştırma konusundaki adsorpsiyon yeteneklerini araştırmaktadır. Azo boyalar sınıfından olan BR 46, tekstil endüstrisinden kaynaklanan yaygın kirleticiler arasında yer almakta olup, yüksek toksisiteleri ve kalıcılıkları nedeniyle ciddi ekolojik ve sağlık riskleri oluşturmaktadır. Mevcut giderim yöntemleri, boya bileşimi, pH ve diğer kirleticiler gibi faktörlerden etkilenerek verimlilik sorunlarıyla karşılaşmaktadır. Gelişmiş oksidasyon işlemleri (AOP'ler) ve adsorpsiyon yöntemleri umut vadetmekle birlikte, pratik uygulama için optimizasyon gerekliliği devam etmektedir. İki boyutlu geçiş metali karbür/nitrür yapılarından oluşan MXeneler, yüksek adsorpsiyon kapasitesi ve kimyasal stabiliteleri sayesinde dikkat çekmektedir. Bu çalışmada, titanyum alüminyum karbür (Ti_3AlC_2) MAX fazı, lityum florür (LiF) ve hidroklorür asit (HCl)

kullanılarak pul pul dökülmüş ve $Ti_3C_2T_x$ elde edilmiştir. Elde edilen malzemenin özelliklerini değerlendirmek amacıyla Fourier Dönüşümü Kızılötesi Spektrometresi (FTIR), X-Işını Kırınımı (XRD) ve Taramalı Elektron Mikroskobu (SEM) gibi karakterizasyon teknikleri kullanılmıştır. Çalışmada, pH, MXene dozajı ve başlangıç boya konsantrasyonu gibi reaksiyon koşullarının BR 46 adsorpsiyonu üzerindeki etkileri incelenmiştir. Sonuçlar, $Ti_3C_2T_x$ MXene'in etkili bir adsorban olduğunu ve atık sulardan toksik boyaların giderilmesinde potansiyel bir çözüm sunduğunu ortaya koymaktadır. Bu araştırma, su kaynaklarındaki boya kirliliğini azaltmaya yönelik verimli, maliyet etkin ve sürdürülebilir yöntemlerin geliştirilmesine katkı sağlamaktadır.

Anahtar Kelimeler: MXene; adsorpsiyon; azo boya; LiF/HCl

1. Introduction

Dyestuffs, particularly azo dyes, are significant pollutants in aquatic environments, originating mainly from textile dyeing processes [1,2]. Azo dyes, constituting a large portion of commercial dyes, are highly toxic due to the presence of mutagenic nitro groups, leading to the generation of harmful byproducts like 1,4-phenylenediamine and o-tolidine [1]. These dyes adversely impact aquatic ecosystems by inhibiting photosynthesis, reducing dissolved oxygen levels, and disrupting the behavior and reproduction of aquatic organisms [2,3]. Furthermore, they can bioaccumulate, entering the food chain and posing serious health risks to both aquatic life and humans [4]. Continuous monitoring of azo dyes in water sources is crucial due to their widespread application and environmental persistence, emphasizing the necessity for effective removal methods to mitigate their ecological implications [1].

Developing effective treatment methods for removing dyestuffs pollutants, particularly azo dyes, from water sources is crucial due to the severe environmental and health risks they pose [5]. Traditional wastewater treatments have limitations, necessitating the exploration of AOPs like photocatalysis and supercritical water oxidation for efficient dye degradation and removal [6]. While these processes are effective, adsorption methods have emerged as an alternative due to their high removal efficiency, ease of operation, cost-effectiveness, and recyclability of adsorbents [7]. Adsorption is particularly advantageous for industries like textiles, where wastewater often contains high levels of color, total dissolved solids, and hazardous metals [8].

Current methods for removing dyestuffs such as BR 46 face several challenges [9]. Physico-chemical methods are influenced by factors like the chemical composition of the dye, pH, temperature, and the presence of other pollutants, impacting the efficiency of removal [10]. AOPs such as using non-thermal plasma reactors have shown promising results but often require complex setups and high-energy inputs [9]. By contrast, adsorption methods are more straightforward, offering the potential for selective dye removal using efficient and inexpensive nano-adsorbents [11]. Heterogeneous Fenton-like catalysts and carbon-silica composites have been explored, but challenges remain regarding catalyst deactivation and the disposal of exhausted materials [12,13]. These limitations highlight the need for innovative adsorbents that address these issues.

MAX phases are a family of layered ternary carbides and nitrides with the general formula $M_{n+1}AX_n$, where M is an early transition metal, A is an A-group element, and X is carbon or nitrogen. Combining the best properties of metals and ceramics, they exhibit exceptional fracture toughness, high strength, hardness, and damage tolerance, enabling resistance to mechanical stresses. Their unique layered structure, with altering metallic (M), group element (A), and carbon/nitrogen (X) layers, underpins these remarkable characteristics [14].

MXenes, initially synthesized in 2011 by etching MAX phases with HF to achieve their unique accordion-like structure and mixed surface terminations (–OH, –O, –F) [15], have since been produced through safer and scalable methods [16]. In 2014, Ghidiu et al. introduced a safer approach using in-situ synthesis of HF by combining LiF and HCl, which both etches the MAX precursor and improves experimental safety [17]. In this study, the Ti_3AlC_2 MAX phase was exfoliated using in situ synthesis of HF by combining LiF and HCl, a safer and more cost-effective method, to synthesize $Ti_3C_2T_x$. MXenes have unique properties like a large specific surface area, good electrical conductivity, and tunable interlayer spacing [18]. These characteristics make them highly efficient for pollutant adsorption, including dye contaminants, and valuable materials for adsorption studies [19].

Adsorption presents several advantages over other treatment methods for removing dyestuffs like BR 46, including simplicity, cost-effectiveness, and the potential for adsorbent recyclability. In this study, the adsorption process was selected over AOPs because of its operational simplicity, lower energy requirements, and suitability for large-scale applications. Many characterization methods FTIR, XRD, and SEM were applied to the synthesized MXene material to evaluate its adsorption performance under varying conditions (pH, MXene dose, and initial BR 46 concentration). The study aims to explore the potential of $Ti_3C_2T_x$ MXene as an efficient and sustainable adsorbent for removing BR 46, addressing current gaps in knowledge and offering a cost-effective solution for wastewater treatment.

2. Materials and Methods

2.1. Materials

Ti_3AlC_2 (known as MAX Phase Micron Powder with an average particle size of 325 Mesh and a purity of more than 99 percent) was acquired from Nanografi. The dye BR 46 was sourced from DyStar and utilized in its as-received state without undergoing any purification processes. Reagent-grade water was generated using a Millipore Milli-Q Ultrapure Gradient 3 V purification setup. LiF, sodium hydroxide (NaOH), HCl, sulfuric acid (H_2SO_4), and ethanol were purchased from Sigma Aldrich, Merck, and ISOLAB respectively.

2.2. Characterization Studies

XRD analysis was conducted using the PANalytical Empyrean XRD instrument, FTIR was performed with the Jasco FT/IR 6700 from Jasco Inc., the SEM utilized was the Hitachi SU3500, and UV/Vis spectrophotometry was carried out using the PerkinElmer UV/Vis Lambda 365 instrument.

2.3. The Synthesis Procedure of MXene

$Ti_3C_2T_x$ MXene synthesis was carried out following methods adapted from the literature [20,21]. Ti_3AlC_2 (1 g) MAX phases were subjected to reaction with 1.88 g LiF and 28 mL HCl (33.13%) for 57 hours at a temperature of 60 °C within a water bath (GFL Shaking Water Bath 1083). The resulting mixture underwent centrifugation (Nüve 400 NF) for 5 minutes at 4100 rpm, following which the supernatant was carefully decanted before introducing 25 mL of deionized water and ethanol into the suspension. Subsequent centrifugation steps were carried out at 4100 rpm for 30 minutes until the pH of the supernatant reached approximately 7. The dispersed sample was then placed in 100 mL ethanol and subjected to sonication (FS-300N Ultrasonic Homogenizer) for 20 minutes under a nitrogen atmosphere. Post-sonication, the sample was dried in a vacuum oven at 60 °C for 24 hours.

2.4. Adsorption Procedure

In the batch adsorption experiments, the effects of the solution's initial pH, the amount of adsorbent, and the initial dye concentration on the removal efficiency of BR 46 dye were analyzed. The dye solutions were prepared at the desired concentrations by diluting a stock solution. After adjusting the pH of the prepared dye solutions, specific amounts of adsorbent were added, and the mixtures were placed in an orbital shaker (Gallenkamp) at a constant temperature and agitated at 180 rpm. Samples were taken at predetermined intervals and centrifuged using a Nüve 400 NF centrifuge at 4100 rpm for 2 minutes to separate the solid and liquid phases. The absorbance of the liquid samples was measured with a PerkinElmer UV/Vis Lambda 365 spectrophotometer, and dye concentrations were determined using a previously established calibration curve. The initial phase of the adsorption experiments investigated the effect of pH on dye removal by varying the pH levels while keeping other parameters constant. The pH was adjusted to the desired levels using dilute H_2SO_4 and NaOH solutions. Next, the effect of different amounts of adsorbent was studied to understand its impact on dye removal. Finally, the influence of the initial dye concentration was assessed at concentrations ranging from 50 to 100 mg/L. The removal rate (R, %) (Eq. 2.1) was calculated using the formula:

$$R\ (\%) = 100 \times \frac{Co - Ct}{Co} \tag{2.1}$$

Where C_0 (mg/L) and C_t (mg/L) are the initial concentration of the solution (mg/L) and the concentration of the solution at time t.

3. Results and Discussion

3.1. Characterization of $Ti_3C_2T_x$

Figure 1 displays the matching XRD patterns of MAX and MXene for comparison. The shift in intensity peak at 37.91° is substantially smaller, suggesting that Al layers in Ti_3AlC_2 can be removed efficiently and with ease [22]. The MAX precursor's strongest signals of 38.69° (104 plane) and 19.08° (004 plane) vanish, and the Al layers are nearly etched away [23]. The planes of Ti_3C_2 (0 0 8), (0 10), and (1 1 0) correspond to the typical peaks (Fig. 1) of Ti_3C_2 at 2θ = 34.65°, 41.79°, and 60.6°, respectively [24].

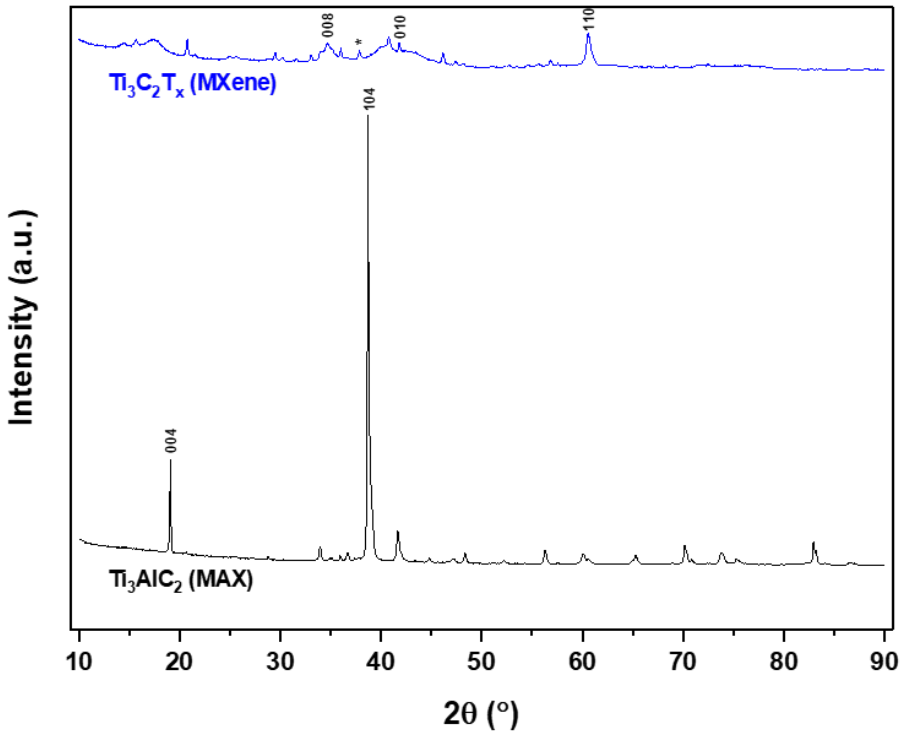

Figure 1. Patterns of Ti_3AlC_2 (MAX) and $Ti_3C_2T_x$ (MXene) X-ray diffraction (XRD)

The SEM pictures of the synthesized $Ti_3C_2T_x$ before and after adsorption are displayed in Figures 2(a) and (b), respectively. As observed in Figures 2(a) and 2(b), the SEM images indicate significant morphological changes before and after the adsorption process. In particular, the etching of the A-layer and the disintegration of the weak M−A connection in the MAX phase result in a unique accordion-like multilayer structure, as seen in Figures 2(a) and (b) [25]. Before adsorption, the $Ti_3C_2T_x$ surface exhibits a well-defined layered structure. After adsorption, the layered structure appears slightly more compacted or obscured, possibly due to the coverage of dye molecules (BR 46) on the surface. These changes confirm the effective interaction of BR 46 dye with the active sites on the $Ti_3C_2T_x$ surface, suggesting successful adsorption and structural modification during the process.

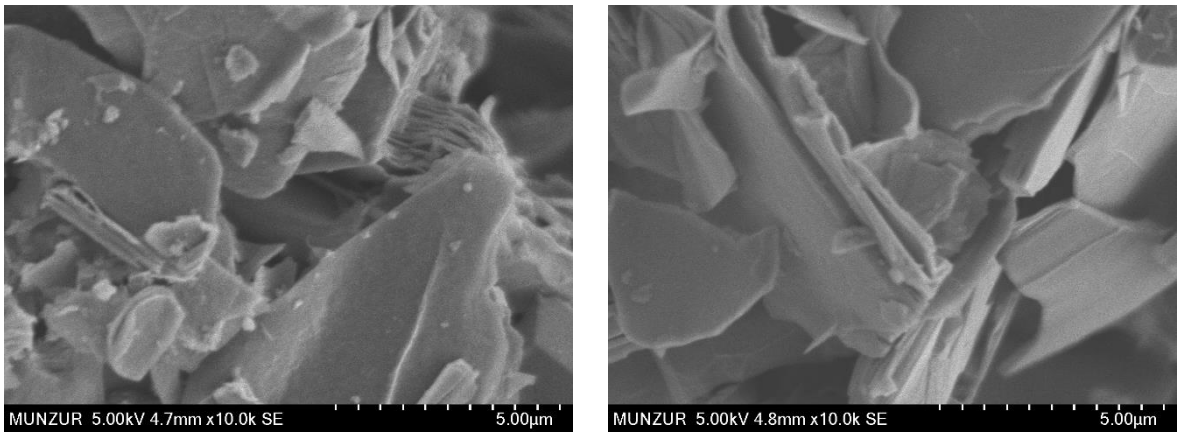

(a) (b)

Figure 2. SEM pictures of $Ti_3C_2T_x$ (a) before adsorption and (b) following adsorption

The FTIR spectra of $Ti_3C_2T_x$ before and after BR 46 adsorption (Fig. 3) highlight the presence of key functional groups on the MXene surface. The peak at 3045 cm^{-1} before adsorption is attributed to O-H stretching, confirming the presence of hydroxyl groups on the material surface. The strong O=C=O stretching peak at 2322 cm^{-1} before adsorption suggests the existence of carboxyl or related functional groups, which are protonated at low pH, enhancing electrostatic interactions with BR 46 molecules. After adsorption, the O=C=O peak shifts to 2363 cm^{-1}, reflecting interactions between the dye molecules and the MXene surface. Additionally, the peak at 582 cm^{-1} corresponds to C-Cl stretching, validating the successful synthesis of $Ti_3C_2T_x$ through LiF+HCl etching. The appearance of a strong C-Br stretching peak at 575 cm^{-1} after adsorption indicates a chemical interaction between BR 46 and the MXene material, further supporting the adsorption process.

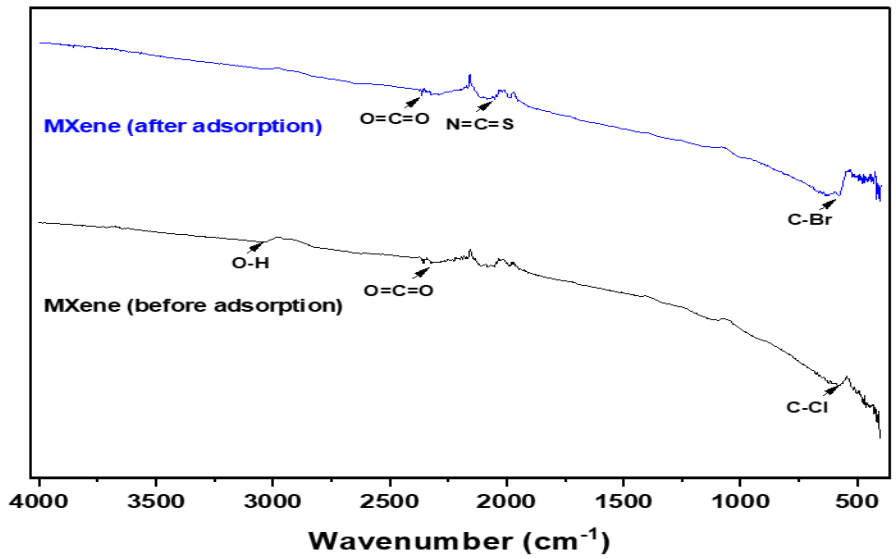

Figure 3. The $Ti_3C_2T_x$ FTIR spectra both before and following BR 46 adsorption

3.2. Adsorption performance of $Ti_3C_2T_x$ on BR 46

3.2.1. Effect of initial pH

The experiment was conducted with an initial concentration of 50 mg/L of BR 46 and a pH between 2 and 11. Figure 4 illustrates the effect of initial pH on the adsorption efficiency of BR 46 dye, with the natural pH of the solution measured at approximately 5.5. The results show that adsorption efficiency is highest at pH 2, where nearly 100% removal is achieved in a short period. As the pH increases, adsorption efficiency generally decreases, consistent with the protonation and deprotonation behavior of the surface functional groups. This was caused by the material's surface's reactive functional groups, like hydroxyl and carboxyl groups, being protonated at low pH. In the meanwhile, H^+ and BR 46 in the solution were competently adsorbed by BR 46, a cationic dye [26]. However, an anomalous dip in adsorption efficiency is observed at pH 7, where the lowest removal efficiency occurs. $Ti_3C_2T_x$'s adsorption effectiveness on BR 46 exhibited a slight upward trend between pH 7.0 and pH 11.0. This was mostly caused by the $Ti_3C_2T_x$ surface hydroxyl groups gradually deprotonating as the pH rose. $Ti_3C_2T_x$ and positively charged BR 46 were able to interact more electrostatically as a result of the increased negative charges on its surface [27]. For the experiments that followed, pH 2 was selected because of its great adsorption effectiveness.

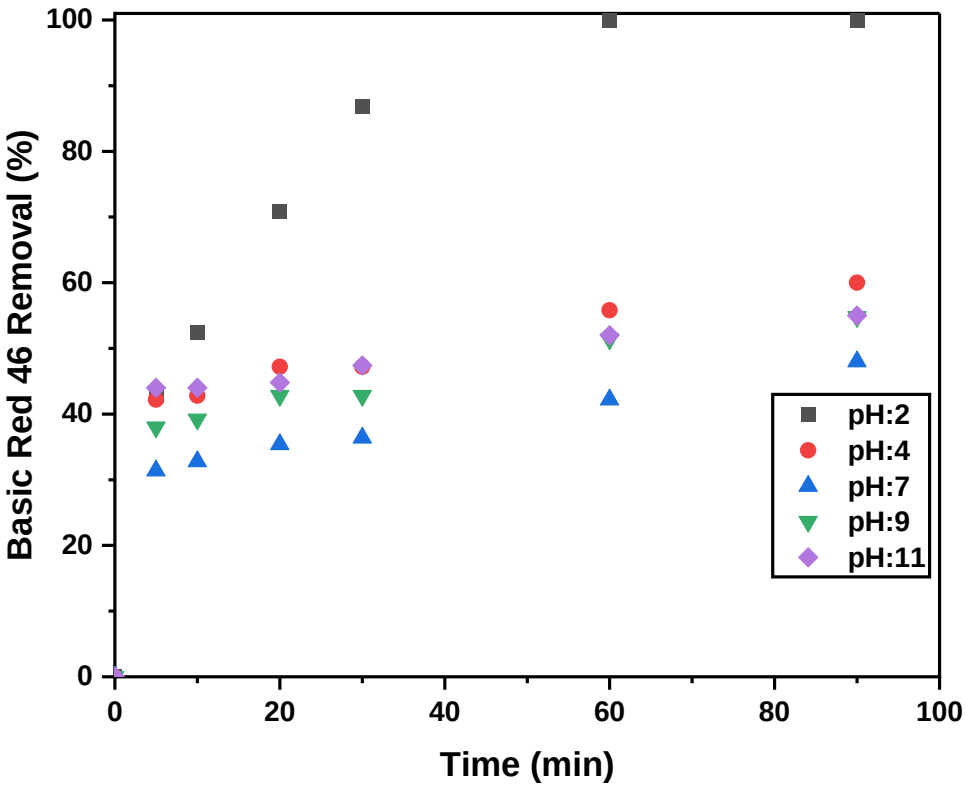

Figure 4. Effect of the solution pH on BR 46 adsorption by $Ti_3C_2T_x$ (conditions: BR 46 concentration = 50 mg/L, temperature = 25ºC, and MXene concentration = 2 g/L)

3.2.2. Effect of MXene dosage

To investigate how adsorbent dosage affected the adsorption process, 1, 2, 4, 6, and 8 g/L of MXene were sequentially added to the solution under the following conditions: 50 mg/L initial BR 46 concentration at 25 °C, 90 min of adsorption contact time. Up until a certain point, Figure 5 illustrates how improving the MXene dosage enhances the adsorption efficiency [28]. A dose of 2 g/L of MXene was optimum. As seen in Figure 5, the adsorption efficiency does not increase significantly beyond this dosage. Similarly, it has been reported that as the adsorbent dosage increases beyond a certain point, the adsorption intensity remains constant, and the adsorption amount becomes independent of the adsorbent dose [29]. At 2 g/L, the adsorption sites on MXene reached saturation, which caused the adsorption efficiency to flatten. No discernible improvement was achieved when additional MXene was added since it did not increase the number of accessible sites for BR 46 to adsorb [30]. For the next experiment, a 2 g/L MXene dosage was used based on the economy and adsorption efficiency.

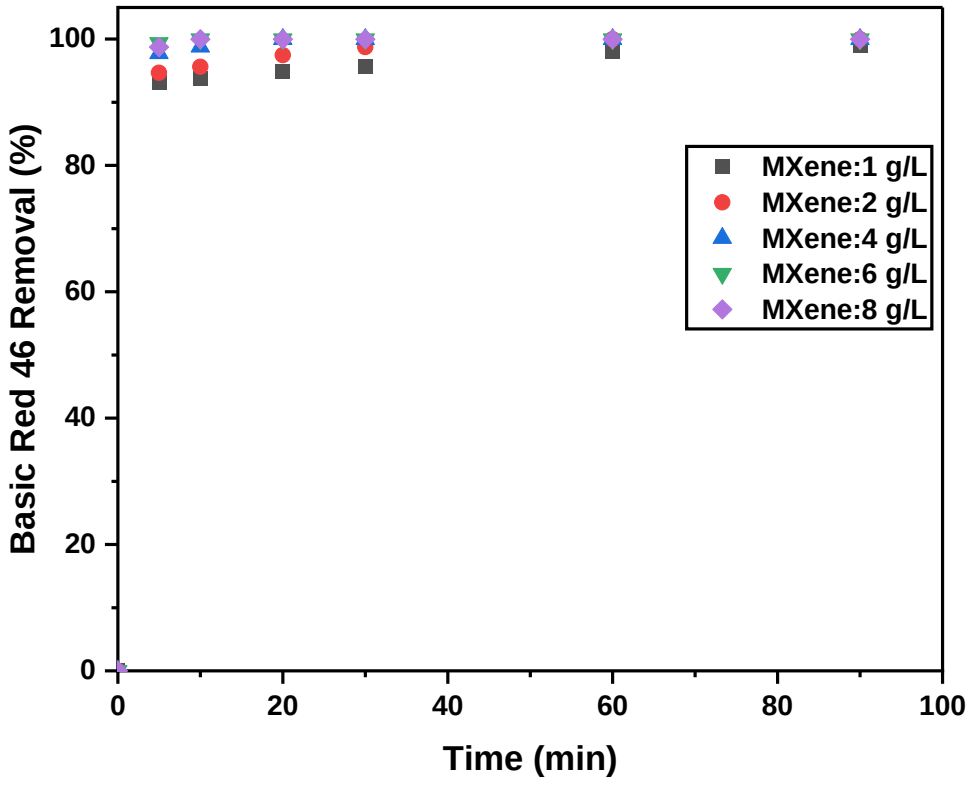

Figure 5. Effect of the MXene dosage on BR 46 adsorption by $Ti_3C_2T_x$ (conditions: BR 46 concentration = 50 mg/L, temperature = 25ºC, and pH = 2)

3.2.3. Effect of initial BR 46 concentration

Figure 6 shows the BR 46 removal efficiency with MXene versus time for initial BR 46 concentrations of 50, 75, and 100 mg/L. Experiments were performed under constant conditions (MXene dosage: 2 g/L; pH: 2; temperature: 25 °C). Higher initial concentrations of BR 46 achieved higher

removal percentages over time. Equilibrium adsorption capacity increased with higher initial concentrations of BR 46 (Table 1). This is seen as the adsorption capacity reaches higher values at higher initial concentrations. This suggests that the adsorption process is driven by the presence of active sites on MXene and the concentration gradient [31]. Higher initial concentrations have also been shown to enhance the driving force of the concentration gradient, facilitating faster diffusion of the adsorbate to the adsorbent surface and increasing the adsorption capacity until saturation is reached [32].

Table 1. *The equilibrium uptake capacities and adsorption efficiencies obtained at different initial BR 46 concentrations*

C_0 mg/L	q_e mg/g	Adsorption (%)
50	24.99	99.98
75	37.19	99.16
100	47.05	94.1

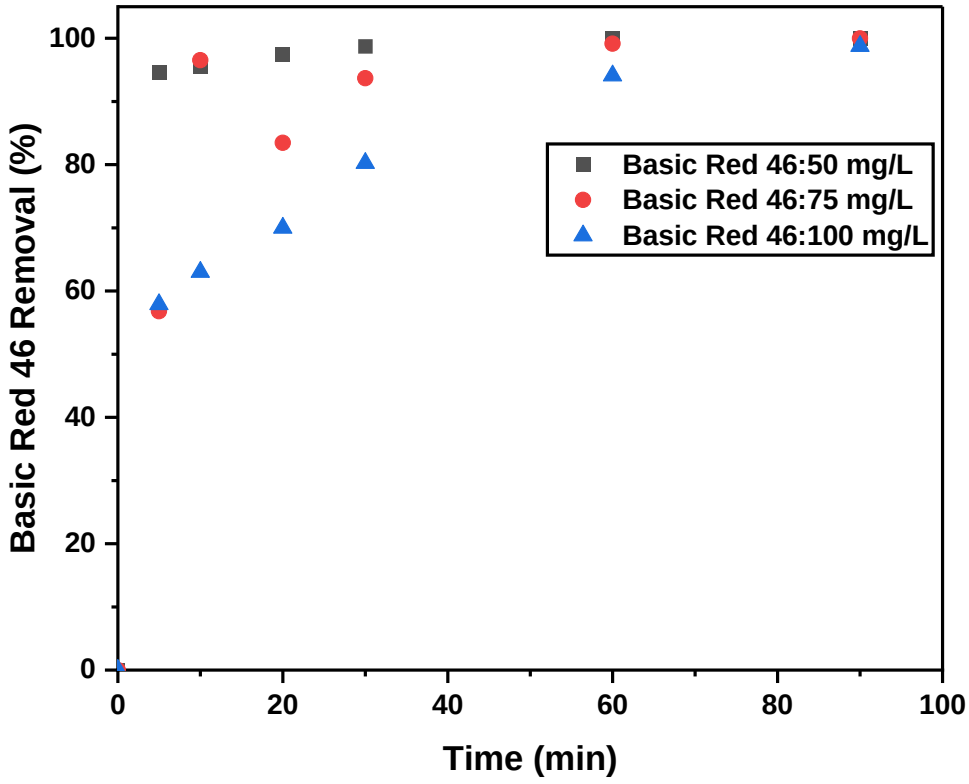

Figure 6. Effect of initial BR 46 concentration on BR 46 adsorption by $Ti_3C_2T_x$ (conditions: MXeneconcentration = 2 g/L, temperature = 25 ºC, and pH = 2)

4. Conclusions

This study successfully demonstrates the high adsorption capacity of $Ti_3C_2T_x$ MXene for the removal of BR 46 dye from aqueous solutions. The synthesis of $Ti_3C_2T_x$ from the Ti_3AlC_2 MAX phase using LiF+HCl was confirmed through FTIR, XRD, and SEM characterization, showing the formation of a typical accordion-like multilayer structure conducive to adsorption. Maximum BR 46 removal efficiency of 99.98% was achieved under optimal conditions of pH 2, 2 g/L $Ti_3C_2T_x$ dosage, 50 mg/L BR 46 concentration, and 60 min contact time. The findings of the study highlight the potential of $Ti_3C_2T_x$ MXene as a highly effective adsorbent in removing toxic dyes from wastewater and offering a promising solution for environmental pollution control. The high adsorption efficiency, stability, and relatively simple synthesis of MXene make it a suitable option for practical applications in wastewater treatment.

Conflict of Interest

The Authors report no conflict of interest relevant to this article.

Research and Publication Ethicts Statement

The authors declare that this study complies with research and publication ethics.

References

[1] Hashemi, S. H., & Kaykhaii, M. (2022). Azo dyes: sources, occurrence, toxicity, sampling, analysis, and their removal methods. In *Emerging freshwater pollutants* (pp. 267–287). Elsevier.

[2] Chadha, P., Mehra, S., & Singh, M. (2021). Adverse impact of textile dyes on the aquatic environment as well as on human beings. *Toxicology International (Formerly Indian Journal of Toxicology)*, 165–176.

[3] Mojiri, A., Zhou, J. L., KarimiDermani, B., Razmi, E., & Kasmuri, N. (2023). Anaerobic membrane bioreactor (AnMBR) for the removal of dyes from water and wastewater: progress, challenges, and future perspectives. *Processes*, *11*(3), 855.

[4] Lekhak, U. M. (2023). Ecotoxicity of synthetic dyes. In *Current Developments in Bioengineering and Biotechnology* (pp. 45–67). Elsevier.

[5] Khan, M. D., Singh, A., Khan, M. Z., Tabraiz, S., & Sheikh, J. (2023). Current perspectives, recent advancements, and efficiencies of various dye-containing wastewater treatment technologies. *Journal of Water Process Engineering*, *53*, 103579.

[6] Vaiano, V., & De Marco, I. (2023). Removal of azo dyes from wastewater through heterogeneous photocatalysis and supercritical water oxidation. *Separations*, *10*(4), 230.

[7] Dutta, S., Gupta, B., Srivastava, S. K., & Gupta, A. K. (2021). Recent advances on the removal of dyes from wastewater using various adsorbents: A critical review. *Materials Advances*, *2*(14), 4497–4531.

[8] Periyasamy, A. P. (2024). Recent Advances in the Remediation of Textile-Dye-Containing Wastewater: Prioritizing Human Health and Sustainable Wastewater Treatment. *Sustainability*, *16*(2), 495.

[9] Abdollahi Ghahi, N., Nohekhan, M., Rezazadeh Azari, F., Rezaei Fard, B., Bakhtiari Ramezani, M., Beigmohammadi, N., Aghamiri, S. Z., & Abdollahi Dargah, M. (2022). Degradation of basic red 46 dye from color wastewater using cold atmospheric plasma. *Journal of Nuclear Research and Applications*, *2*(4), 21–24.

[10] Ganaie, R. J., Rafiq, S., & Sharma, A. (2023). Recent advances in physico-chemical methods for removal of dye from wastewater. *IOP Conference Series: Earth and Environmental Science*, *1110*(1), 12040.

[11] Islam, A., Teo, S. H., Taufiq-Yap, Y. H., Ng, C. H., Vo, D.-V. N., Ibrahim, M. L., Hasan, M. M., Khan, M. A. R., Nur, A. S. M., & Awual, M. R. (2021). Step towards the sustainable toxic dyes removal and recycling from aqueous solution-A comprehensive review. *Resources, Conservation and Recycling*, *175*, 105849.

[12] Rial, J. B., & Ferreira, M. L. (2021). Challenges of dye removal treatments based on IONzymes: Beyond heterogeneous Fenton. *Journal of Water Process Engineering*, *41*, 102065.

[13] Wiśniewska, M., Chibowski, S., Wawrzkiewicz, M., Onyszko, M., & Bogatyrov, V. (2022). CI Basic Red 46 removal from sewage by carbon and silica based composite: equilibrium, kinetic and electrokinetic studies. *Molecules*, *27*(3), 1043.

[14] Alam, M. S., Chowdhury, M. A., Khandaker, T., Hossain, M. S., Islam, M. S., Islam, M. M., & Hasan, M. K. (2024). Advancements in MAX phase materials: structure, properties, and novel applications. *RSC Advances*, *14*(37), 26995–27041.

[15] Naguib, M., Kurtoglu, M., Presser, V., Lu, J., Niu, J., Heon, M., Hultman, L., Gogotsi, Y., & Barsoum, M. W. (2011). Two-dimensional nanocrystals produced by exfoliation of Ti3AlC2. In *MXenes* (pp. 15–29). Jenny Stanford Publishing.

[16] Huang, P., & Han, W.-Q. (2023). Recent advances and perspectives of lewis acidic etching route: an emerging preparation strategy for MXenes. *Nano-Micro Letters*, *15*(1), 68.

[17] Ghidiu, M., Lukatskaya, M. R., Zhao, M.-Q., Gogotsi, Y., & Barsoum, M. W. (2014). Conductive two-dimensional titanium carbide ‘clay’with high volumetric capacitance. *Nature*, *516*(7529), 78–81.

[18] Gopalram, K., Kapoor, A., Kumar, P. S., Sunil, A., & Rangasamy, G. (2023). MXenes and MXene-Based Materials for Removal and Detection of Water Contaminants: A Review. *Industrial & Engineering Chemistry Research*, *62*(17), 6559–6583.

[19] Irfan, S., Khan, S. B., Din, M. A. U., Dong, F., & Chen, D. (2023). Retrospective on Exploring MXene-Based Nanomaterials: Photocatalytic Applications. *Molecules*, *28*(6), 2495.

[20] Maleski, K., Mochalin, V. N., & Gogotsi, Y. (2017). Dispersions of two-dimensional titanium carbide MXene in organic solvents. *Chemistry of Materials*, *29*(4), 1632–1640.

[21] Alhabeb, M., Maleski, K., Anasori, B., Lelyukh, P., Clark, L., Sin, S., & Gogotsi, Y. (2017). Guidelines for synthesis and processing of two-dimensional titanium carbide (Ti3C2T x MXene). *Chemistry of Materials*, *29*(18), 7633–7644.

[22] Demirelli, K., Barim, E., Çelik, A., Yegin, M., Aksoy, Y., Hanay, Ö., & Hasar, H. (2024). Photoresponse, thermal and electrical behaviors of MXene-based polysulfone nanocomposite. *Polymer Bulletin*, 1–22.

[23] Yan, P., Zuo, Z., Hou, M., Zhao, S., & Zhang, Z. (2023). MXene/nano-sized carbide-derived carbon composite with enhanced supercapacitive performance in acidic electrolyte. *Ionics*, *29*(1), 411–418.

[24] Lu, X., Zhu, J., Wu, W., & Zhang, B. (2017). Hierarchical architecture of PANI@ TiO2/Ti3C2Tx ternary composite electrode for enhanced electrochemical performance. *Electrochimica Acta*, *228*, 282–289.

[25] Wang, R., Cao, H., Yao, C., Peng, C., Qiu, J., Dou, K., Tsidaeva, N., & Wang, W. (2023). Construction of alkalized MXene-supported CoFe2O4/CS composites with super-strong adsorption capacity to remove toxic dyes from aqueous solution. *Applied Surface Science*, *624*, 157091.

[26] Yan, J., Liu, P. F., Wen, H. X., & Liu, H. J. (2022). Effective Removal of Basic Red 46 with Ti3C2 Powder Modified with Citric acid. *ChemistrySelect*, *7*(29), e202201733.

[27] Li, Z., Li, J., Tan, J., Jiang, M., Fu, S., Zhang, T., & Wang, X. (2022). In situ synthesis of novel peroxo-functionalized Ti3C2Tx adsorbent for aqueous pollutants removal: Role of oxygen-containing terminal groups. *Chemosphere*, *286*, 131801.

[28] Humelnicu, D., Ignat, M., & Suchea, M. (2015). Evaluation of Adsorption Capacity of Montmorillonite and Aluminium-pillared Clay for Pb 2+, Cu 2+ and Zn 2+. *Acta Chimica Slovenica*, *62*(4).

[29] Nezami, S., Ghaemi, A., & Yousefi, T. (2024). Experimental exploring of Ti3C2Tx MXene for efficient and deep removal of magnesium in water sample. *Scientific Reports*, *14*(1), 27508.

[30] Sen, N., Shefa, N. R., Reza, K., Shawon, S. M. A. Z., & Rahman, M. W. (2024). Adsorption of crystal violet dye from synthetic wastewater by ball-milled royal palm leaf sheath. *Scientific Reports*, *14*(1), 5349.

[31] Basu, S., Ghosh, G., & Saha, S. (2018). Adsorption characteristics of phosphoric acid induced activation of bio-carbon: Equilibrium, kinetics, thermodynamics and batch adsorber design. *Process Safety and Environmental Protection*, *117*, 125–142.

[32] Li, J., Dong, X., Liu, X., Xu, X., Duan, W., Park, J., Gao, L., & Lu, Y. (2022). Comparative study on the adsorption characteristics of heavy metal ions by activated carbon and selected natural adsorbents. *Sustainability*, *14*(23), 15579.